

Investigation of the Liquid Phase Sintering of Size Range Composed Powder for SLS Application

Klas Boivie

Woxéncentrum, KTH, The Royal Institute of Technology, Sweden

Abstract

In order to find the constraints and limiting factors for the development of a series of homogenous steel materials has three different aspects of such a material system been investigated in relation to each other; the composition of powders, the formation of green bodies and sintering in a vacuum furnace. It was found that particle size range intervals must be optimised, not only in respect to maximum part precision and powder density but also to interparticle friction and laser penetration. Sintering time and temperatures should be adapted to particles shape and diffusion rates, as well as the possible evaporation of alloy components. Furthermore should the fraction of melting phase be balanced between solubility of liquid agent in base material and the wetting of solid particles as well as being integrated in the smaller sized fraction of the powder composition. While these issues remain undetermined, the possibility for parts of homogenous steel materials by SLS cannot be eliminated.

1. Introduction

Among the most widely used systems for powder based metallic application of SFF technology, are different metallic applications to laser sintering, Direct Metal Laser Sintering, (DMLS) by EOS, and metallic material SLS by 3D Systems. Both systems have several traits in common, however one fundamental difference is that while EOS uses a powerful laser to consolidate the material by point wise liquid phase sintering in the machine, 3D Systems uses a two step approach where the metallic consolidation by solid state sintering and infiltration takes place in a separate furnace. However, as the metallic applications of SFF technology have been gaining momentum for the purpose of prototyping and small series manufacturing over the last few years, there has been a growing interest to expand the capacity into production grade tooling and fully functional metallic parts. Since objects made of various steel alloys traditionally have fulfilled many of these applications, the possibilities for the SFF application of a variety of homogenous steel materials, from traditional tools steels to stainless steels, is an area of obvious interest. Therefore, a material system that would allow the building of objects in homogenous steel materials, would if applied to a process that is well established on the market, greatly expand the possible applications of SFF technology, and thereby make a significant contribution to bridge the gap between conventional practice and SFF technology.

The two-step SLS based process, in combination with Liquid Phase Sintering (LPS), has been suggested as an alternative route to make full density objects. As one way of exploiting this possibility, Rockwell sciences center has developed a set of (LPS) materials, under the name of Direct Metal Fabrication (DMF)[1]. However in this process is the debinding of the green bodies as well as a substantial shrinkage during sintering critical issues. One possibility to minimize the shrinkage while sintering to full density, is to compose the powder of selected particle sizes where each smaller fraction fills the voids between the larger particles, thereby

acquiring the highest possible fraction of solids in the powder mass [2], [3]. Some practical aspects and limitations high-density powder composition in relation to SLS equipment have been investigated in a previous work [4]. However any addition of organic binders to the powder blend would decrease the density of metal particles. But since the reactivity of the powder particles increase with smaller particle size, there is a distinct possibility that the smaller particles could be stimulated to bond to the larger particles and thus act as a metallic binder. However, to reach a homogenous material by LPS, the liquid phase must be completely integrated with the base material after full density has been reached, one possible way to achieve this is to use a liquid phase that slowly dissolves into the other powder components.

It is the purpose of this present work to investigate this approach to the development of a family of steel materials for SLS application. The basic principle is to use blend of small sized powders, consisting of a melting phase material with the capacity to dissolve into iron-based alloys, in this case copper, and an iron powder as filler material. This blend can be combined with a choice of base material steel powder to achieve a variety of steel materials. During sintering, the copper melts, providing the liquid phase for sintering, and a diffusion route for the homogenization of alloy components, while slowly dissolving into the steel material. Since the outcome of approach is dependent on every part of this multi-step process, this investigation takes an over-all approach to finding the limiting factors and monitoring the behavior, from the composition of the powder blends, over the powder application and the formation of green bodies in the Sinterstation, to the final metallic consolidation during the furnace process.

2. Background

2.1 Powder Composition

The density of powder beds been addressed in previous research, both in general, [2], [3], and for SLS technology, by experimental set up [5], and by this author, in a more practical approach by application in a Sinterstation [4]. It was found that given a maximum particle size, the number of additional powder size fractions is limited by the increasing interparticle friction that accompanies the addition of smaller sized particles. When the particle sizes are as small as 1-2 μm , the powder mass is too “sticky” to form acceptable powder layers. Since the size relationship between larger and smaller particles ideally is at least 7:1, [2], [3], it was concluded that powder compositions with more than two size fractions hardly are feasible for Sinterstation application. Furthermore, it was found that the powder spreading system in the Sinterstation has a positive densifying effect on the applied layer, unless the interparticle friction in the powder mass dominates over the free flowing behavior, then the effect is opposite.

Since copper is well established as a liquid phase, in conventional powder metallurgy [2], [10], with the capacity to dissolve into iron base alloys and with positive effects on for example strength and corrosion resistance, copper is the choice of melting phase in this investigation. An even distribution of the liquid phase is important for LPS purposes therefore should the copper particles be intermixed among the smaller sized particles. An early investigation into the SLS aspects of the Fe-Cu-C LPS system [11], concluded the importance of loose powder density, and also registered some effects of the copper amounts and presence carbon on the sintering behavior. Following up, a primary investigation much similar to this [6],

took these aspects in consideration while composing powder blends by combination of iron-based powders with a small sized copper covered iron powder. However since the smaller particle size had been determined by an approximation of the powder material surface assuming spherical shape, the particle size was different from powder specification. This resulted in a much lower powder density than expected, which made sintering to full density impossible. Nevertheless, metallic bonded green bodies were formed. This present investigation, while taking these experiences in respect, looks further into the behavior of the materials during the formation of green bodies and furnace processing.

2.2 Formation of Green Bodies

In the previously mentioned primary investigation [6] metallic bonded green bodies were formed in a Sinterstation, using a moderate laser power and low scanning speeds. Much research along the same lines for the iron copper material system has been performed at the Katholieke Universiteit, Leuven, [7], [8], [9], however mostly in the aspect of the powder spreading mechanism [7] and laser interaction with powder material [8]. Apparently aiming at LPS by laser exposure, these efforts have not been directed towards maximizing powder mass density. Aiming at homogenous steel material by furnace consolidation is the applied powder density and the arrangement of particles in the green body is of critical importance in this present work. However improving the strength of green bodies, pointwise melting and solidification causes thermal tensions and distortions in each layer. Therefore is the melting of copper and LPS at laser exposure not necessarily desirable for this approach, however it may turn out to be unavoidable.

2.3 Sintering

The Fe-Cu system for LPS is well known in conventional powder metallurgy and has consequently also been the subject for research with the aspect of combination with SLS [6], [9], [11]. However none of these investigations has taken the diffusion of copper into the base material into real consideration. Copper dissolves into iron base alloys by substitution, which is a slow process and thereby allowing prolonged LPS. This could possibly offer the opportunity to control the sintering behavior by the combination of particle sizes with the amount of copper and sintering temperature to achieve a homogenous material within reasonable sintering times. Another critical limiting factor for the sintering behavior is the oxidation of the powder. In order to reduce the inevitable oxides, and provide a reliable atmosphere [2], is a vacuum furnace atmosphere suitable for the sintering operation. However, certain essential alloying elements, for example Cr can evaporate during vacuum processing at high temperatures [12], which put a serious constraint to the process temperatures in this approach. This will be taken into consideration while determining the process parameters.

3. Calculations

The time and temperatures for the furnace procedure in order to achieve a homogenous material are controlled by some important boundary conditions. The temperature must be high enough, and process time must be long enough to allow the complete dissolving of copper into the base material, as well as the homogenization of all other alloying components. However vacuum furnace processing temperatures are limited by the risk of evaporation alloying components from the material, thus placing an upper limit on the temperatures, while the times are limited primarily by the competitiveness of the process. The time to dissolve the copper into the base material is controlled by the fractional saturation of copper in the base material particles. Darken & Gurry [13] gives us the relationship:

For diffusion into spherical shape: $Dt/L^2 = -0.05043 - 0.2333 \log(1 - F)$, [Eq. 1]

Diffusion constant, $D = D\gamma_{Cu}^{Fe} = 1.8 \exp\left(-295 kJmol^{-1}/RT\right) cm^2/s$, [Eq.2]

Fractional saturation, $F = \frac{C_m - C_0}{C_s - C_0}$, [Eq.3], and L is the diffusion distance, here the radius of the

base material particles which in the case of $-44\mu m$ powder is 0.00225 cm. For saturation this gives [Eq. 1] $Dt/L^2 = 0.9$. At $1120^\circ C$ is $D\gamma_{Cu}^{Fe} = 1.56 \cdot 10^{-11} \Rightarrow 81.13$ h, which is too long.

In a similar manner are the times to saturation at $1200^\circ C \Rightarrow 19.89$ h, at $1250^\circ C \Rightarrow 9.23$ h, and at $1300^\circ C \Rightarrow 4.3$ h. However, the upper temperature limit is determined by the evaporation of critical alloying components during vacuum processing. Since stainless steel is one material of particular importance in this investigation, the evaporation of chromium is of critical importance during the sintering operation [12]. Gas pressure equilibrium can be calculated from the known

relationship $\ln p_1 - \ln p_2 = -\frac{\Delta H_m}{R} \left[\frac{1}{T_1} - \frac{1}{T_2} \right]$ [Eq. 4], [12], where index "1", is referring to the

triple point equilibrium, and index "2" to process conditions. This gives: $p_1 = 1 atm \Rightarrow \ln p_1 = 0$, for chromium: $T_1 = 2620 + 273 = 2893K$, $\Delta H_m = 81.7 \cdot 10^3 cal \cdot mol^{-1}$, and

$R = 1.987 calK^{-1}mol^{-1}$. Assuming standard vacuum furnace settings ($p = 4.94 \cdot 10^{-7} atm$) and ideal gas behavior, chromium gas pressure of the selected stainless steel alloy (22.4% Cr, $\Rightarrow X_{Cr} = 0.2357$), will be $p_2 = 2.096 \cdot 10^{-6} atm$, inserted in [Eq. 4] this gives the gas pressure equilibrium temperature for this alloy in a vacuum furnace $T_2 = 1506.78K \Rightarrow 1233.6^\circ C$.

Therefore should the process temperature not be much higher than $1200^\circ C$, though sintering times of close to 20 h at $1200^\circ C$ would lead to unreasonable process times. However a slight reduction in copper content, from equilibrium at approx. 9% to 8%, would change the fractional saturation value, [Eq. 3] to 0.888, which in turn gives [Eq. 1] $Dt/L^2 = 0.17$ which would give a process time of 3.85 h, a much more reasonable value.

4. Experimental

4.1 Powder Composition

Since the powder mass is going to be densified by addition of smaller sized particles, and the experiments are aiming at achieving homogeneity after completed sintering, the alloy of the base material will be diluted. In order to maintain some of the desirable properties, it is suitable that the base materials powder is slightly over-alloyed. For the purpose of this experiment two different base powders selected, one tool steel, Anval 9044, see **Fig. 1. & Tab1.** and one stainless steel, Anval 2205, see **Fig. 2. & Tab2.** Both base material powder were of $-44\ \mu\text{m}$ particle size.

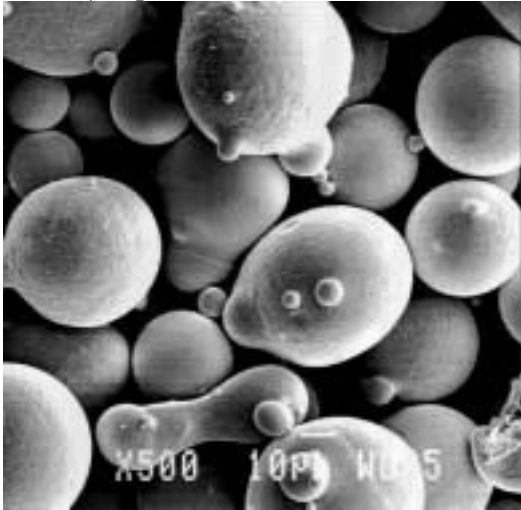


Fig.1. Anval9044. An alloyed tool steel material, with the characteristic spherical shape of gas atomized metal powder. The spherical shape is known to have the lowest interparticle friction and thus the best possible flowing behavior and packing. Size analysis: ASTM-E11 sieve, 88 % < $-45\ \mu\text{m}$.

C	Si	Mn	P	S	Cr	Ni	Mo
1.31	0.65	0.41	0.018	0.02	4.2	0.13	5.1

Nb	Cu	Co	V	Sn	W	N	O
0.01	0.08	0.1	3.10	0.01	6.65	0.06	70

Table 1. The chemical composition of the tool steel base material, Anval 9044.

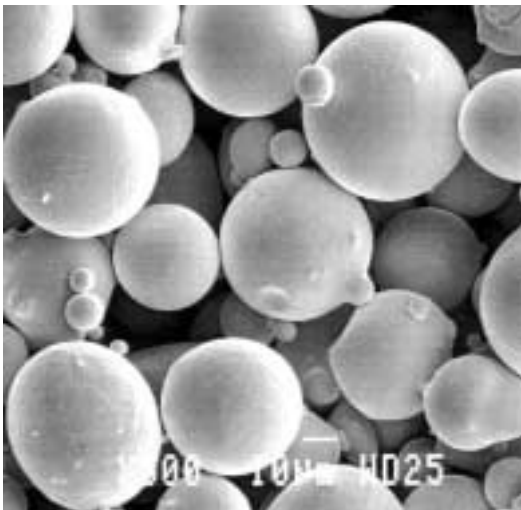


Fig.2. Anval2205. A stainless steel material, with the characteristic spherical shape of gas atomized metal powder. This alloy has been selected in order to maintain some desirable properties, should it reach full density after sintering. Size analysis: ASTM-E11 sieve, 91 % < $-45\ \mu\text{m}$

C	Si	Mn	P	S	Cr	Ni	
0.017	0.68	1.11	0.017	0.001	22.4	5.19	

Mo	Nb	Cu	Co	V	W	N	O
3.00	0.01	0.14	0.03	0.07	0.02	0.18	110

Table 2. The chemical composition of the stainless steel base material, Anval 2205, O in ppm.

As the melting copper phase, a fine sized copper powder from Micron Metals, “Cu-110, 99.9%, spherical 1-5 micron” was selected, see **Fig. 3.**, however, both the particle size and shape had apparently been evaluated by approximative method. The particles were considerable larger, thus out of the suitable size range for densification, and also of sponge like constitution. This will most likely have a less than positive effect on the densification of the powder mass when added to the base powder.

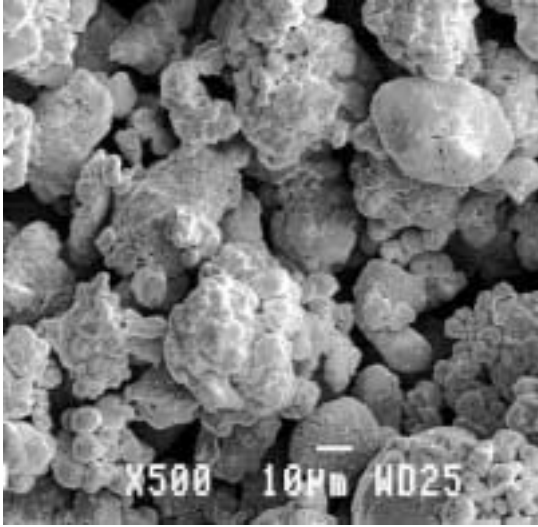


Fig.3. Copper powder, 99.9% Cu. According to vendor 1-5 μm spherical shape, which in reality obviously is not the case. This discrepancy is however most likely due to the method of measuring and calculating size. In many cases are such small sized particle's sized estimated by a measured value for particle surface that is recalculated to volume and diameter assuming spherical shape. For a sponge like powder such as this, this method would indicate a much smaller particles size than really is the case. For this investigation will this defect disturb the size range composition and thus limit the density improvement.

The filler material, particles to fit into the voids between the base material particles and melting phase particles, were a carbonyl iron powder, “Carbonyl SM” see **Fig. 4. & Tab.3.** This powder, of very small sized particles, has very high inner friction due to van der Waal's and electrostatic forces, which will have a significant influence on the powder behavior.

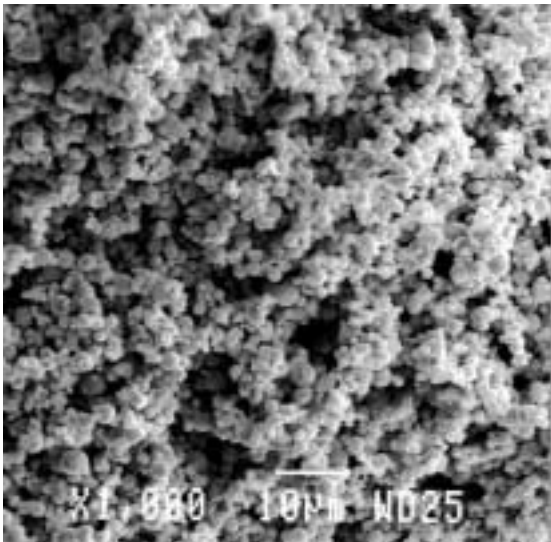


Fig.4. Carbonyl Iron SM: almost pure iron, with the spherical shape typical of carbonyl metal powder. In this size range (2-8 μm), the interparticle friction is associated with van der Waal's and electrostatic forces, and is thus increasingly independent of particle shape. Nevertheless, the spherical shape still is the best possible considering the achievable packing properties.

Fe	C	O	N
Min. 99.0	Max. 0.2	Max. 0.8	Max. 0.1

Table 3. The chemical composition of the filler material, Carbonyl SM.

The composition of the different powders for optimization of particle density was determined by the same experimental procedure as described in [4]. However since the amount of copper has been settled at 8%, the variation in composition concerned base and filler material. The sampled tap densities of different powder compositions showed little variation, which suggests that the internal friction, (and probably also the less than perfect shape of the copper particles) has a significant influence on the behavior of powder composed of these powders. Still, a composition of 75% base material, 17% Carbonyl SM and 8% copper was found to have a modest maximum of tap density for both base materials, 63.3% for Anval 2205, and 66.3% for Anval 9044. However, after a few trials in the Sinterstation, the internal powder friction, was found to be to high, and the composition was modified to consist of 77% Anval 2205, 15% Carbonyl SM and 8% copper. Assuming that the present oxygen is in the shape of metal oxides and to ensure the deoxidizing of the material during vacuum processing, was a small addition of graphite made to the powder compound. Thus, the investigated powder compositions were:

Anval 2205 I	
Anval 2205	74.91%
Carbonyl SM	16.98%
Cu	7.99%
Graphite	0.107%

Anval 2205 II	
Anval 2205	76.99%
Carbonyl SM	15.00%
Cu	8.00%
Graphite	0.097%

Anval 9044	
Anval 2205	74.92%
Carbonyl SM	16.98%
Cu	7.99%
Graphite	0.106%

4.2 Formation of Green Bodies

Build file: The software used in this experiment was slightly manipulated versions of standard material files for this equipment. Since this investigation required the option to vary a number of variables, such as laser powers and scanning speeds, a material file for DTM's Duraform material was used, although this limits the powder layer thickness not to be smaller than 0.08 mm, which probably is thicker than optimal for this application. Since the metallic bonded green bodies in previous work has been known to curl in each layer, [6], [8], was one of the parts integrated in the build file a 10 mm thick mesh structure in which the other parts were partially embedded. This piece, while curling slightly, anchored the parts in the surrounding powder and thus acted as a support, until the formed green body was rigid enough to resist the curling effect, see **Fig. 5**.



Fig. 5. Support mesh and parts in position. The powder is spread in this picture's left-right direction.

Powder application: Initial trials were used to investigate the spreading behavior and to determine the suitable powder deposition variables, following the same procedure as in [4]. It was found that, while tap densities for the Anval 2205 I and Anval 9044 blends had been well above 63%, the applied densities of these blends barely reached 61%. Since the applied powder layers, especially for Anval 2205, also had a small tendency to crack at the surface, a behavior typical for powders with too high inter particle friction, it was concluded that the combination of these powders, despite only two size range components and altogether smooth and spherical particle shapes, still involves too much interparticle friction to arrange in a favorable manner in the Sinterstation.

Test 1. Anval 2205 I: Fine but very brittle metallic bonded green bodies were formed using fill laser powers 25–35 W, fill scan speeds 450–500 mm/s, outline laser power 25 W, outline scan speed 600 mm/s, and layer thickness 0.08 mm, see **Fig. 6**. Monitoring the powder bed's behavior during scanning, it was noted that some rearrangement of powder apparently took place, and that the green body, apart from some curling, occurring from layer 2 until approximately 5 mm build height, tended to rise slightly from the surrounding powder mass.

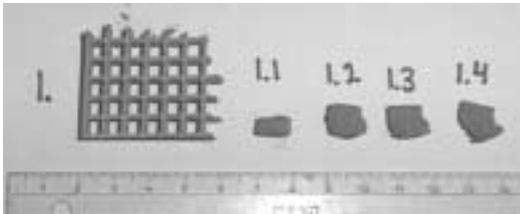


Fig. 6. Metallic bonded green bodies. Test 1. 1; Fill laser power: 35W, fill scan speed:500. 1.1; Fill laser power: 25W, fill scan speed:450. 1.2; Fill laser power: 30, fill scan speed:450 1.3; Fill laser power: 32.5W, fill scan speed:450. 1.4; Fill laser power: 35W, fill scan speed:450. Outline laser power:25W, outline scan speed 600, for all.

Test 2. Anval 2205 II: More curling and slightly stronger green bodies were formed using the new powder composition, fill- and outline laser powers 30-35 W, and fill- and outline scanning speeds 400-450 mm/s. Similar powder orientation behavior as in the previous test was noted, see **Fig. 7**. However, the applied powder density was raised to 64.6%.

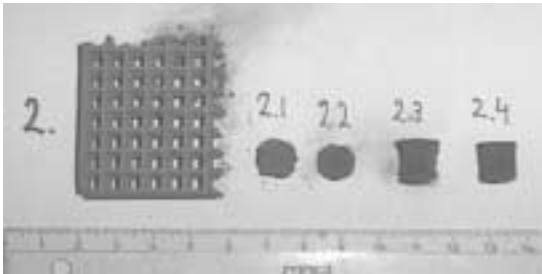


Fig. 6. Metallic bonded green bodies. Test 2. 2; Laser power: 35W, scan speed:400. 2.1; Laser power: 30W, scan speed:400. 2.2; Laser power: 30, scan speed:450 2.3; Laser power: 35W, scan speed:400. 2.4; Laser power: 35W, scan speed:450. Fill and outline parameter settings are identical for the same part.

Test 3. Anval 9044: The further increase of laser powers: fill- 35-40 W, outline laser power 30-37 W, and decrease in scanning speeds: fill- 350-400 mm/s, and outline scanning speed 300-370 mm/s, relative to the previous tests, has further increased orientation and curling. However, the green bodies were strong enough to be handled and cleaned without breakage despite thin sections, see **Fig. 8**. It is also noted that the bonds in each layer is considerable stronger than the bonds between layers. Meanwhile, the surface quality along the outlines decreases with increased exposure to laser energy.

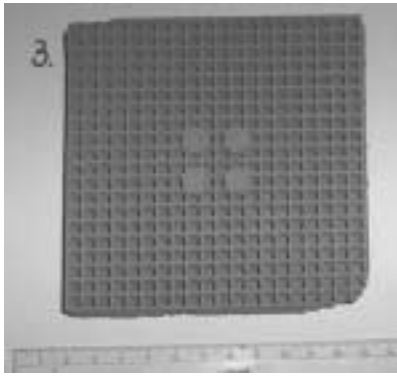


Fig. 8. Test 3. Laser power variation 32-40W and scan speed 300-400. Some initial curling and adherent movement during application of new layers. Small difference between parts, though a tendency to curl and brake out of position for pieces exposed to higher laser energy. Stable enough to be rinsed and handled in one piece.

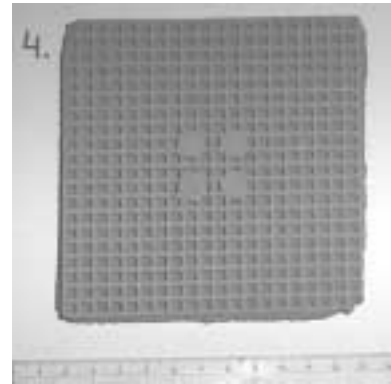


Fig. 9. Test 4. Laser power variation 30-40W and scan speed 250-350 Displays a similar behavior as in Test 3 (**Fig. 8.**) Though stronger green bodies, the tendency for curling shifting and for pieces to brake out of position is more obvious.

Test 4. Anval 9044: At these levels laser power, fill- 35-40 W, outline- 30-37 W and scanning speeds fill- 300-350 mm/s, outline- 250-320 mm/s, is the curling se severe, and the green bodies so strong that the first layers, up until approximately 6 mm, shifts and moves with the passing of the roller. While the green bodies were strong, the surface quality along the outline was rather poor, see **Fig. 9**.

SEM micrographs of the green bodies' surfaces reveal further information about the powders' behavior during the SLS processing see **Fig. 10, 11, & 12**. The powder has not been arranged in any favorable manner, which confirms the negative influence of interparticle friction. Apparently, a fraction of the powder has melted, and since copper is the powder blend component with the lowest melting temperature, it is reasonable to assume that the melted part is copper. Furthermore, it appears, as the smallest particles are arranged closer together, opening wider pores as the green bodies had been exposed to more laser energy (**Fig. 10. & 12.**). This implies that there has been some sort of rearrangement among the smaller particles, which has been dependent on heat exposure.



Fig. 10. Test 1. Green body surface of support mesh, laser power 35w scan speed 500.

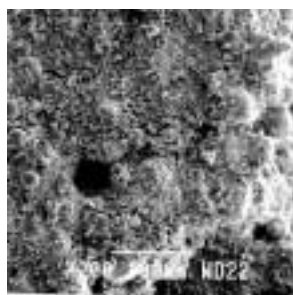


Fig. 11. Test 2. Green body surface of support mesh, laser power 35w scan speed 400.



Fig. 12. Test 4. Green body of support mesh, laser power 40w scan speed 350.

4.3 Sintering

Furnace procedure: The green bodies were sintered in a conventional vacuum furnace in accordance with calculations and the principles described in [12]. The temperature was raised to 1200 °C at a rate of 200 °C/h, held at this temperature for 4 h, when the temperature was lowered at the same rate. The parts were placed on an alumina powder bed, in a graphite crucible, with no surrounding powder for support.

Result: Some sintering and thus shrinkage took place, see **Fig. 13, 14, 15 & 16**, however not to full density and significant porosity remained in all parts, see **Fig. 17, 18 & 19**. Green bodies that had been subjected to a higher laser energy were more rigid and maintained their shape better, including overhangs, during sintering, whereas the weaker bonded green bodies tended to sag under their own weight. The porosity is mainly oriented along the layers and laser scanning paths, and appears to be more severe if the green bodies were formed with a higher laser power, **Fig. 17 & 18**. This could be an effect of the particle orientation observed in the green bodies.

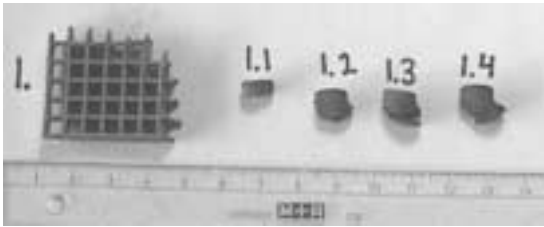


Fig. 13. Test 1. Sintered.

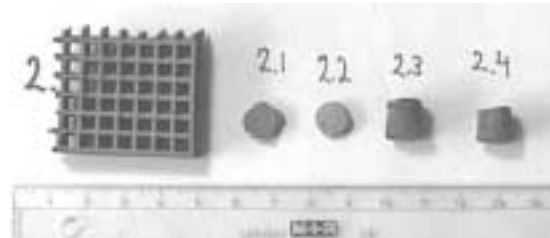


Fig. 14. Test 2. Sintered.

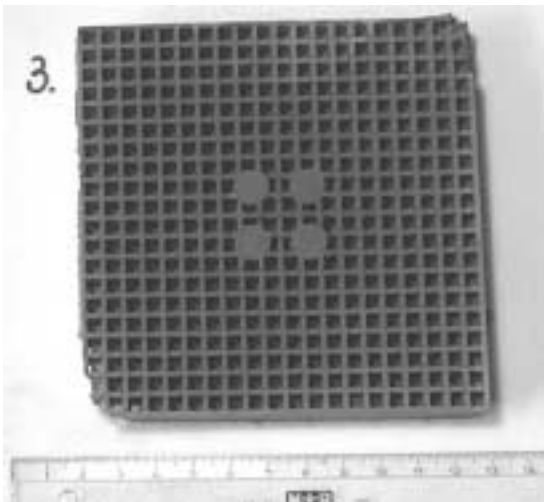


Fig. 15. Test 3. Sintered.

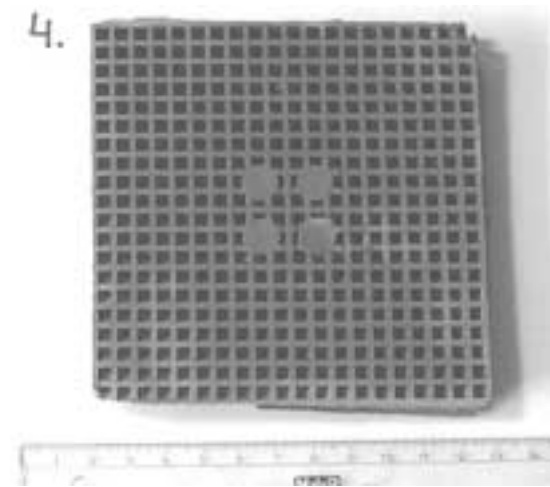


Fig. 16. Test 4. Sintered.

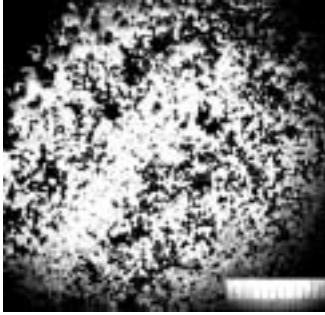


Fig. 17. Anval 2205, part 1.2, top view slightly angled to building direction. Slightly etched in 1 part ferric chloride, 10 parts hydrochloric acid & 20 parts water. Scale: 1 unit = 0.01 mm. Notice how the porosity has been positioned in between the layers.

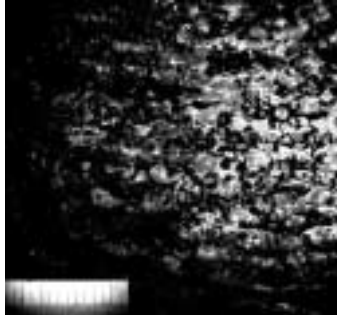


Fig. 18. Anval 9044, sample from Test 4, side view, perpendicular to building direction, etched in 4% Nital solution. Some carbide particles are visible, but more important is the severe porosity, oriented in streaks along the slightly curved layers.

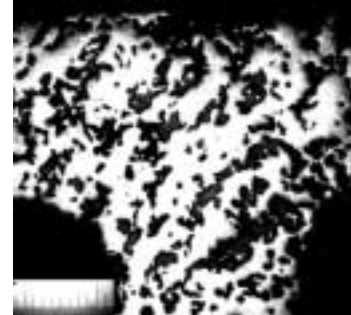


Fig. 19. Anval 9044 support mesh from Test 4, top view, building direction, slightly etched in 4% Nital solution. The angle of the porosity streaks is parallel to the laser scanning direction.

5. Discussion and Conclusions

Despite being composed by powder within the size range interval determined in [4], it appears that the interparticle friction is too high to reach any higher powder packing densities, though the achievable powder densities was further limited by the copper particles' deviation from the expected size and shape. Nevertheless, interparticle friction is dependent on the particle size of all particles in the powder blend, and it is likely that improved powder performance could be achieved by using larger particles for the base material, both in respect to interparticle friction and the less than perfect copper particles. However, this solution would prolong the sintering times to dissolve all the liquid material and could also make thicker layers necessary, and thus obstruct the laser heat penetration and bonding to the underlying layer.

The green bodies were joined by metallic bonds. Partially by of surface diffusion, but as it appears, mostly by the melting of copper particles, not at all unlike brazing. If so, it can also be concluded that the principal cause for the curling of the layers is the shrinking of copper during solidification. With the copper melted, it is further reasonable to assume that some liquid phase sintering is in progress at this stage, which would account for the increased green strength and curling of the green bodies at increased laser powers and slower scanning speeds. Furthermore, this could explain a part of the rearrangement of particles noted. Rearrangement is caused by surface diffusion, and occurs normally at the initial stage of sintering [2], and normally leads to densification. However, in this case the powder particles are arranged with local areas of higher density while there are other areas of lower density. Since the liquid copper only seems to wet a fraction of the particles, this causes uneven LPS, for a brief period of time. Meanwhile, the surface diffusion strives to straighten the points of contact between particles, which will cause a movement among the small sized particles, which has been known to widen large pores in areas

of already low density [14]. This effect is also known to increase with smaller particle sizes and could have affected the behavior during the furnace process.

This effect could have been further enhanced by the laser formation of metallic bonded green bodies. Since the exposed areas have been subjected to a higher thermal impact, the melted material has been concentrated to these areas, likewise braze in a brazing operation. Areas that have not directly been exposed to the laser have thus only sintered and bonded by heat conduction. The new layers have been applied to surfaces with oriented particles, and the points of contact with the previous layer have not been directly exposed to the laser and therefore have weaker bonding. When the green bodies are processed in the furnace the sintering has been directed by the particle orientation, and there has not been enough liquid phase to wet all surfaces simultaneously to compensate for this and allow complete pore closure.

This investigation was aimed at finding the principal limiting factors, to form solid parts from a variety of homogenous steel materials by LPS of SLS shaped green bodies using size range composed powder. While this possibility cannot be eliminated at this stage, there are some difficulties to come to terms with.

1. Powder composition: The particle size ranges of the different powders should fulfill certain criteria to allow the application with high density in a Sinterstation. Apart from particle shape and size proportions there are smallest acceptable sizes for base material (larger particles) as well as fill material and melting phase, (smaller size range). The adverse effect of interparticle friction caused by small sized particles is well known. However, the size of the larger particles is a principal limiting factor for the layer thickness, which is important not only for part precision but also for laser energy penetration and therefore also a determining factor for the green strength. This is obviously a matter for optimization.
2. Sintering time and temperatures: To achieve homogeneity in the material, the sintering time must be long enough and temperatures must be high enough to permit the homogenization by diffusion of all materials. One critical variable for this is the largest particles' size. Diffusion rates increases with increased temperatures, however dependent on the base material there are upper practical limits for the sintering temperatures. For most traditional tool steels, these are determined mainly particle coarsening and melting temperatures. In the present tool steel this would probably allow processing at somewhat higher temperature than used in this investigation. Stainless steels are due to evaporation of important alloying components, more sensitive to high temperatures during vacuum furnace processing, and would require a different strategy to reach full density.
3. The fraction of melting phase: Despite no apparent segregation of copper in the applied powder material and long sintering time, there has been a concentration of liquid copper to certain areas during the laser- and subsequent furnace treatment. The liquid phase during the furnace sintering has not been sufficient, by amount and/or distribution to wet all surfaces and stimulate pore closure in the whole green body. But if homogeneity is to be achieved, copper levels are limited by the solubility in the base material during sintering. Therefore, one likely way for further investigation of this possibility would be to identify another suitable liquid phase material with the capacity to dissolve into the

base material. But even so, will that material have to be successfully integrated in the powder, particularly in regard to powder density and spreading characteristics as well as interaction with the laser.

References

1. <http://www.rsc.rockwell.com/structuralmaterials/index.html>
2. German R.M. "Powder Metallurgy Science", MPIF 1994.
3. McGeary, R.K., "Mechanical Packing of Spherical Particles," J. Am. Ceramic Soc., 1961, vol. 44, pp. 513-522.
4. Boivie, K, "Limits of Loose Metal Powder Density in the Sinterstation" Bourell, D.L., et al., editors, Proceedings of the Solid Freeform Fabrication Symposium 2001, The University of Texas at Austin 2001.
5. Karapatis, N, et al. "Optimization of Powder Layer Density in Selective Laser Sintering" Bourell, D.L., et al., editors, Proceedings of the Solid Freeform Fabrication Symposium 1999, The University of Texas at Austin 1999, pp 255-263.
6. Boivie, K, "Investigation of Size Range Composed Powder For SLS Based Liquid Phase Sintered Tooling" Dimitrov, D., editor, Proceedings of the 2nd Annual Conference on Rapid Technologies 2001, The University of Stellenbosch 2001.
7. Van der Schueren, B, and Kruth, J.P. "Powder Deposition in Selective Metal Powder Sintering" Rapid Prototyping Journal, 1995, vol. 1, Nr 3, pp. 23-31.
8. Kruth, J.P. et al. "Direct Laser Sintering of Steel/Cu Without Polymer Binder: a Comparison between CO₂ Nd:YAG lasers. Katholieke Universiteit Leuven, 1998.
9. Bonse, J. "Selective Laser Sintering of Metal Powders" Ph.D. Thesis, Jan. 2001. Katholieke Universiteit Leuven, 2001.
10. Le May, I et al. "Copper in Iron and Steel" John Wiley & Sons, 1982.
11. Boivie, K, "SLS Application of the Fe-Cu-C System for Liquid Phase Sintering" Bourell, D.L., et al., editors, Proceedings of the Solid Freeform Fabrication Symposium 2000, The University of Texas at Austin 2000.
12. Boivie, K, "A Vacuum Furnace Process for DTM's RapidSteel 2.0 Material" Bourell, D.L., et al., editors, Proceedings of the Solid Freeform Fabrication Symposium 1999 The University of Texas at Austin 1999.
13. Darken, L.S. and Gurry, R.W. "Physical Chemistry of Metals" McGraw-Hill 1953.
14. Runfors, U. "Powder metallurgy", Dep. of Physical Metallurgy, KTH, Sweden 1987. (Swedish)